Identification of delays and discontinuity points of unknown systems by using synchronization of chaos

Francesco Sorrentino
Università degli Studi di Napoli Parthenope, 80143 Napoli, Italy
and University of Maryland, College Park, Maryland 20742, USA

(Received 24 December 2009; revised manuscript received 22 March 2010; published 24 June 2010)

In this paper, we present an approach in which synchronization of chaos is used to address identification problems. In particular, we are able to identify (i) the discontinuity points of systems described by piecewise dynamical equations and (ii) the delays of systems described by delay differential equations. Delays and discontinuities are widespread features of the dynamics of both natural and manmade systems. The foremost goal of the paper is to present a general and flexible methodology that can be used in a broad variety of identification problems.

DOI: 10.1103/PhysRevE.81.066218 PACS number(s): 05.45.Xt

I. INTRODUCTION

A technique to reconstruct the full state vector of a chaotic system from the time series of a single observed scalar was proposed in [1]. Recent work [2–4] has shown that synchronization of chaos can be used as a powerful tool to identify the dynamical equations of unknown systems. For instance, in [4] a largely unknown chaotic system was coupled to a model system and an adaptive strategy was proposed to make them synchronize by adaptively varying the parameters of the model until they converge on those of the true system. This strategy relies on the assumption that the equations of the true system can be written as linear combinations in a set of unknown scalar parameters $\{a_i\}$,

$$\dot{x}(t) = \sum_i a_i \lambda_i[x(t)], \tag{1}$$

where $x(t)$ is the known n-state of the system at time t, $\lambda_i : R^n \rightarrow R^n$ is a set of known (non)linear functions of x (an analogous description of the dynamics can be considered for discrete time systems).

The case of Eq. (1) is also considered in Ref. [3], where a general *linear independence condition* is presented that needs to be satisfied in order to identify the parameters of interest. The references in Ref. [2] propose a technique to reconstruct the parameters of unknown chaotic systems in both computer simulations and experiments from knowledge of their dynamical time evolution. Yet, the problems of identification of unknown delays and discontinuity points of chaotic systems have received little attention so far.

An important observation is that in terms of our proposed problem, dealing with chaotic systems represents an advantage; in fact, since a chaotic time trace never repeats in time, it provides an infinite amount of information that can be used by the identification strategy. On the other hand, a disadvantage is that stability of synchronization of chaotic systems is usually evaluated locally about the synchronized evolution and for the parameters of the systems being the same (i.e., it relies on the successfulness of the identification strategy). Therefore, the effectiveness of the strategy may be sensitive to the choice of the initial conditions and it may depend on a careful selection of the adaptive strategy parameters.

Chaos can arise in systems whose dynamics is described by delay dynamical equations or by piecewise linear and piecewise differentiable equations. These are both very common situations in nature and in applications. For example, piecewise dynamical equations characterize mechanical systems with impacts [5], relay-feedback systems [6], and dc/dc converters [7]. Delay dynamical equations are usually invoked to describe physiological processes in hematology, cardiology, neurology, and psychiatry [8]; but find application also in chemistry, engineering and technological systems [9]; examples are lasers subject to optical feedback [10], high-speed machining [11], mechanical vibrations [12], control engineering [13], and traffic flow models [14]. Our goal is introducing a flexible adaptive strategy that can be used to identify either discontinuity points or delays of the equations of unknown chaotic systems from knowledge of their state evolution. To our knowledge, the use of adaptive strategies to deal with these two interesting and important problems has not been considered yet in the literature (note that adaptive strategies become particularly useful when the unknown parameters to be identified are time dependent). More in general, the paper presents a general methodology that can be used to address a broad variety of identification problems, including apparently difficult ones.

The case of Eq. (1), in which the unknown parameters to be estimated (the $\{a_i\}$) appear in the equations of the unknown system as the coefficients of a linear combination is quite specific. A broader class of problems includes identification of parameters that cannot be written in the form of the a_i in Eq. (1). Estimation of such parameters is the subject of the present paper; in particular, we present two examples in which we deal with estimation of discontinuity points and delays. In Sec. II, we address the problem of identifying discontinuity points of unknown piecewise dynamical systems. In Sec. III, we address the identification of delays of unknown dynamical systems. Finally, in Sec. IV, the conclusions are presented.

II. IDENTIFICATION OF DISCONTINUITY POINTS

In this section, we deal with the problem of identifying discontinuity points of piecewise dynamical systems. We present a fully nonlinear approach that can be used to extract the discontinuity points of these systems from knowledge of their dynamical time evolution. We consider both the cases, in which the unknown true system evolves in discrete and in continuous time.

As a first (simple) *problem*, we consider that the unknown true system is described by a piecewise dynamical equation and evolves in discrete time. In particular, we assume that the unknown system evolution obeys,

$$x^{k+1} = f_{\sigma}(x^k), \tag{2}$$

where $x^k \in R$, $f_{\sigma}(x): R \to R$ is a piecewise differentiable function,

$$f_{\sigma}(x) = \begin{cases} f^{I}(x), & \text{if } g(x) \leq \sigma, \\ f^{II}(x), & \text{otherwise}, \end{cases} \tag{3}$$

where $f^{I}(x): R \to R$, $f^{II}(x): R \to R$, and $g(x): R \to R$ are C^1 functions and σ is a scalar. For simplicity (and without loss of generality), for this first example, we assume that the true system state x is a scalar quantity. The more general case that the state is n dimensional is discussed next for the case of a continuous time system.

Our goal is to identify the unknown parameter σ from knowledge of the temporal evolution x^k. To this aim, we seek to model the dynamics of the true system by

$$y^{k+1} = f_{\sigma'}(\tilde{y}^k), \tag{4}$$

where σ' is an estimate of the unknown true coefficient σ, and $\tilde{y}$ is defined as

$$\tilde{y}^k = \epsilon y^k + (1 - \epsilon) x^k, \tag{5}$$

$\epsilon \in R$. Note that the model is coupled to the true system through x^k in Eq. (5). We proceed under the assumption that the value of ϵ in Eq. (5) is such that when $\sigma' = \sigma$, the synchronized solution $y = x$, is stable. Our strategy (to be specified in what follows) seeks to synchronize the model to the true systems, by dynamically adjusting σ' to match the unknown true value of σ. We now introduce the following *potential*,

$$\Psi = [x - y]^2, \tag{6}$$

$\Psi \geq 0$ by definition; $\Psi = 0$ when $y = x$, that is, when the true system and the model system are synchronized. Thus, we seek to minimize the potential (i.e., to achieve synchronization between the two systems) by dynamically adjusting the estimate σ' through the following gradient descent relation,

$$\sigma'^{k+1} - \sigma'^{k} = -\eta \frac{\partial \Psi}{\partial \sigma'} = 2\eta [x^k - y^k] \frac{\partial y^k}{\partial \sigma'} \equiv 2\eta [x^k - y^k] p^k, \tag{7}$$

$\eta > 0$. We note that the term $p^k \equiv \partial y^k / \partial \sigma'$ appears in Eq. (7); therefore, we seek to find a recurrence equation that describes the evolution of p^k in time. Equation (4) can be rewritten as

$$y^{k+1} = f^{I}(\tilde{y}^k) \mathcal{H}[\sigma' - g(\tilde{y}^k)] + f^{II}(\tilde{y}^k) \{1 - \mathcal{H}[\sigma' - g(\tilde{y}^k)]\}, \tag{8}$$

where $\mathcal{H}$ is the Heaviside step function, $\mathcal{H}(z) = 1$ if $z \geq 0$, 0 otherwise. In what follows, we will seek to compute the derivative of the right hand side of Eq. (8) with respect to σ'. However, the function $\mathcal{H}[\sigma' - g(\tilde{y}^k)]$ is not differentiable with respect to σ' at $\sigma' = g(\tilde{y}^k)$. To overcome this difficulty, we introduce the replacement,

$$d\mathcal{H}(z)/dz \to \delta_{\omega}(z), \tag{9}$$

where $\delta_{\omega}(z)$ is the triangular function,

$$\delta_{\omega}(z) = \omega^{-1} \max(1 - |z/\omega|, 0), \tag{10}$$

$\omega \neq 0$. Note that the replacement Eq. (9) introduces an approximation in the equations of the adaptive strategy [though other approximations are possible, our numerical simulations show that the replacement Eq. (9) is one convenient choice]. In particular, Eq. (9) corresponds to assuming that in the model system the transition between f^{I} and f^{II} occurs continuously as a function of σ' [while the transition is actually discontinuous in Eq. (4)]. However, we note that if the identification strategy is successful, i.e., for $\sigma' = \sigma$, our model [Eq. (4)] is the same as the true system [Eq. (2)], implying that a state of complete synchronization, $y = x$, exists; when this synchronous state is achieved, $\sigma'^{k+1} - \sigma'^{k} = 0$ in Eq. (7), i.e., the adaptive strategy is in turn *deactivated*. Thus, our hope is that though our strategy uses an approximate description of the model system, it will converge onto the desired synchronous state.

By using (9), we can now write the following recurrence equation for p^k,

$$p^{k+1} = a^k p^k + b^k, \tag{11a}$$

with

$$\begin{aligned} a^k = \epsilon \{ & Df^{I}(\tilde{y}^k) \mathcal{H}[\sigma' - g(\tilde{y}^k)] + Df^{II}(\tilde{y}^k) \{1 - \mathcal{H}[\sigma' - g(\tilde{y}^k)]\} \\ & + [f^{II}(\tilde{y}^k) - f^{I}(\tilde{y}^k)] \delta_{\omega}[\sigma' - g(\tilde{y}^k)] Dg(\tilde{y}^k) \}, \end{aligned} \tag{11b}$$

$$b^k = [f^{I}(\tilde{y}^k) - f^{II}(\tilde{y}^k)] \delta_{\omega}[\sigma' - g(\tilde{y}^k)]. \tag{11c}$$

Note that Eq. (11a) is an *auxiliary* difference equation that completes the formulation of our adaptive strategy [described by the set of Eqs. (4), (7), and (11)]. In fact, by iterating the set of Eqs. (4), (7), and (11) and by using knowledge of the time evolution of the true system state x_k, we obtain a time evolving estimate σ' of the unknown quantity σ.

Figure 1 shows the results of a numerical experiment in which Eq. (3) is the tent map equation, $f^{I}(x) = \mu x$, $f^{II}(x) = \mu(1 - x)$, $\mu = 1.4$, and $\sigma = 0.6$. For these values of the parameters, the tent map dynamics is chaotic. Moreover, we choose $g(x) = x$, $h(x) = x$, $\epsilon = 0.4$, and $\omega = 0.1$. We initialize both the true system and the model from uniformly distributed random initial conditions between 0 and 1, and σ' is evolved from an initial estimate that is far away from the true value of σ, i.e., $\sigma'(0) = 0.4$. Figures 1(a) and 1(b) show the time evolutions of x^k (in black, thin line) and y^k (in gray, thick line), respectively, at the beginning ($k \in [0, 50]$) and at the

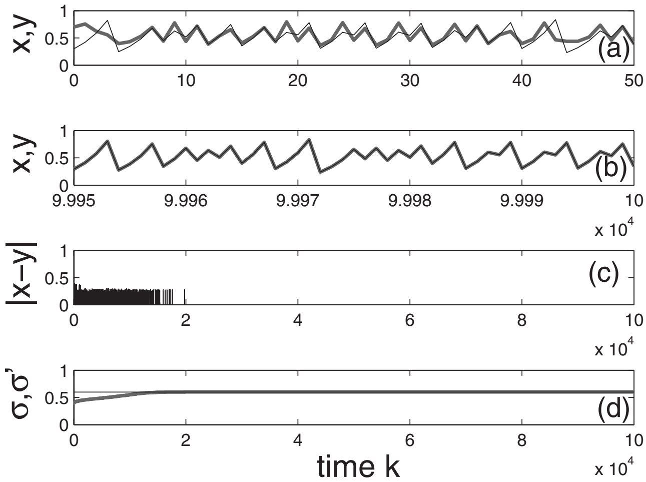

FIG. 1. (a) and (b) show the time evolutions of x^k (in black, thin line) and y^k (in gray, thick line) respectively at the beginning ($k \in [0,50]$) and at the end ($k \in [99\,950,\ 100\,000]$) of the run [in (b) the two curves are superposed]. Plot (c) shows $|x^k - y^k|$ versus k. (d) shows the time evolution of σ'^k (in gray), which converges to the true value of $\sigma=0.6$ (in black, thin line). $f^I(x)=\mu x$, $f^{II}(x)=\mu(1-x)$, $\mu=1.4$, $g(x)=x$, $h(x)=x$, $\epsilon=0.4$, $\eta=10^{-4}$, and $\omega=0.1$.

end ($k \in [99\,950,\ 100\,000]$) of the run [in Fig. 1(b) the two curves are superposed]. Figure 1(c) is a plot of the synchronization error $|x^k - y^k|$ versus k, from which we see that the adaptive strategy is successful in achieving synchronization between the true and the model systems. Figure 1(d) shows the time evolution of σ'^k converging to the true value of $\sigma=0.6$.

We also investigate how the choice of the parameter ω in Eq. (10) affects the identification strategy [Eq. (10) is even in ω, so we will only consider $\omega > 0$]. While our strategy requires $\omega > 0$ in Eq. (10), it is clear that the larger the ω, the worse our model (4) approximates Eq. (2), for $\sigma' \neq \sigma$. Therefore in what follows, we will make use of numerical simulations to test how the choice of ω in Eq. (10) affects the performance of our strategy.

This is shown in Fig. 2(a), where the same simulation in Fig. 1 is repeated as the parameter ω is varied. The equations are integrated for a long time. The thick line is a plot of σ'_f, the final value of σ' estimated by the adaptive strategy at the end of each run, versus ω, while the thin dotted line is the true $\sigma=0.6$-th ordinate line. As can be seen, the strategy is effective in estimating the unknown value of σ, for $10^{-2} \lesssim \omega \lesssim 5 \times 10^{-1}$. An interesting result that we observe is the failure of our strategy for small values of ω. To better understand this phenomenon, we have run other numerical simulations for the case that $\sigma'(0) \approx \sigma$ and we have found that for small values of ω the synchronized solution is unstable with respect to infinitesimal (small) perturbations. Figure 2(b) is a plot of the average synchronization error $\langle |x-y| \rangle$ calculated from integration of Eqs. (2)–(5), versus σ' assumed *constant*, for the case that true value of σ has been set to 0.6. The plotted synchronization error is averaged over a long time and the initial transient, which reflects the choice of the initial conditions, is neglected. As can be seen, the average synchronization error is characterized by a sharp minimum at $\sigma' = \sigma$, and it rapidly increases with $|\sigma' - \sigma|$.

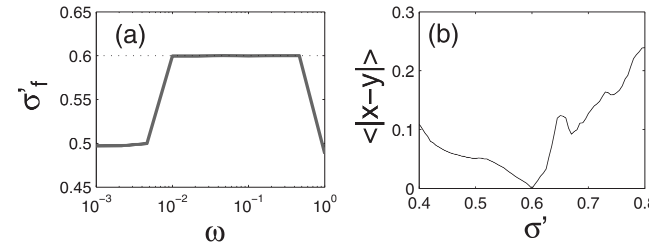

FIG. 2. (a) The same simulation in Fig. 1 has been repeated as the parameter ω is varied. The thick line is a plot of σ'_f, the final value of σ' estimated by the adaptive strategy at the end of each run, versus ω, while the thin dotted line is the $\sigma=0.6$-th ordinate line. (b) is a plot of the average synchronization error $\langle |x-y| \rangle$ calculated from integration of Eqs. (2)–(5), versus σ' assumed *constant*, for the case that true value of σ has been set to 0.6. The plotted synchronization error is averaged over a long time and the initial transient is neglected. All the simulation parameters are the same as in Fig. 1.

As a second *problem*, we consider that the unknown system evolves in continuous time and is n dimensional. We assume that the system dynamics is described by the Chua equation, $n=3$, $\mathbf{x}(t)=[x_1(t),x_2(t),x_3(t)]^T$, $\dot{\mathbf{x}}(t)=F_\sigma[\mathbf{x}(t)]$,

$$F_\sigma(\mathbf{x}) = \begin{Bmatrix} \alpha\{x_2(t) - x_1(t) - \phi_\sigma[x_1(t)]\} \\ x_1(t) - x_2(t) + x_3(t) \\ -\beta x_2(t) \end{Bmatrix}, \tag{12}$$

where the piecewise scalar function $\phi_\sigma(x)$ is defined as,

$$\phi_\sigma(x) = \begin{cases} m_1 x + \sigma(m_0 - m_1), & x \geq \sigma \\ m_0 x, & |x| < \sigma \\ m_1 x - \sigma(m_0 - m_1), & x \leq -\sigma. \end{cases} \tag{13}$$

For our choice of $\alpha=15.6$, $\beta=25.58$, $m_0=-8/7$, and $m_1=-5/7$, the Chua system (12) and (13) displays chaos (the emergence of a chaotic "double scroll" attractor has been observed both in numerical simulations and in experiments [15]). In the case of Eq. (13), the function $\phi_\sigma(x)$ has two discontinuity points, i.e., at $\pm\sigma$. In the general case in which ν discontinuity points are present, ν independent gradient descent relations can be derived for each of the points and simultaneously integrated [together with other ν corresponding *auxiliary* equations, analogous to Eq. (11)] in order to identify them all. Yet, in the case of the Chua system (12), the problem can be simply formulated in the only unknown σ (i.e., we rely on the fact that the two discontinuity points are symmetrical with respect to zero).

We assume to model the true system by $\mathbf{y}(t)=[y_1(t),y_2(t),y_3(t)]^T$, $\dot{\mathbf{y}}(t)=F_{\sigma'}[\mathbf{y}(t)]$, where σ' is an estimate of the unknown true parameter σ. We design an adaptive strategy to dynamically adjust σ' to match the unknown value of σ. To this aim, we perform a one way diffusive coupling from the true system to the model, as follows,

$$\dot{\mathbf{y}}(t) = F_{\sigma'}(\mathbf{y}(t)) + \Gamma[h(\mathbf{x}(t)) - h(\mathbf{y}(t))], \tag{14}$$

where $h(\mathbf{x})$ is in general an $m \leq n$ vector of m observable scalar quantities that are assumed to be known functions of the system state $\mathbf{x}$. Γ is an $n \times m$ constant coupling matrix. In what follows, we assume for simplicity that h is a scalar function ($m=1$), $h(\mathbf{x})=x_1$, and $\Gamma=[\gamma,0,0]^T$, and we proceed under the assumption that the value of γ is such that when $\sigma'=\sigma$, the synchronized solution, $\mathbf{y}=\mathbf{x}$, is stable. We introduce the following potential,

$$\Psi=[h(\mathbf{x})-h(\mathbf{y})]^2. \tag{15}$$

Again, $\Psi\geq 0$ by definition, and $\Psi=0$ if $h(\mathbf{y})=h(\mathbf{x})$, that is, when the true system and the model system are synchronized. Thus, we seek to minimize the potential by adaptively evolving σ' according to the following gradient descent relation,

$$\dot{\sigma}'=-\zeta\frac{\partial\Psi}{\partial\sigma'}=2\zeta[h(\mathbf{x})-h(\mathbf{y})]Dh(\mathbf{y})\frac{\partial\mathbf{y}}{\partial\sigma'}$$
$$\equiv 2\zeta[h(\mathbf{x})-h(\mathbf{y})]Dh(\mathbf{y})\mathbf{q}, \tag{16}$$

$\zeta>0$. Note that for our choice of h, $Dh=[1,0,0]$, yielding $Dh\mathbf{q}=q_1$, where q_1 is the first component of the vector $\mathbf{q}$. Therefore, we seek a differential equation that describes how $q_1\equiv\partial y_1/\partial\sigma'$ evolves in time. We note that $\phi_{\sigma'}$ can be rewritten as,

$$\phi_{\sigma'}(y_1)=m_0y_1+(m_1-m_0)[\mathcal{H}(-\sigma'-y_1)(y_1+\sigma')$$
$$+\mathcal{H}(y_1-\sigma')(y_1-\sigma')]. \tag{17}$$

Then, from Eqs. (14) and (17), we obtain the following *auxiliary* differential equation for q_1,

$$\dot{q}_1(t)=c(t)q_1(t)+d(t), \tag{18a}$$

where

$$c(t)=-\gamma-\alpha\{1+m_0+(m_1-m_0)[\mathcal{H}(-\sigma'-y_1)$$
$$+\mathcal{H}(y_1-\sigma')]\}, \tag{18b}$$

$$d(t)=-\alpha(m_1-m_0)[\mathcal{H}(-\sigma'-y_1)-\mathcal{H}(y_1-\sigma')]. \tag{18c}$$

Our adaptive strategy is then fully described by the set of Eqs. (14), (16), and (18). Figure 3 shows the results of a numerical experiment, in which we have integrated Eqs. (12), (14), (16), and (18). Both the true and the model systems are initialized from uniformly distributed random initial conditions on the Chua chaotic attractor, and σ' is evolved from an initial value that is far away from the true value of $\sigma=1$, i.e., $\sigma'(0)=2.5$, $q_1(0)=0$. Figures 3(a) and 3(b) show the time evolutions of $x_1(t)$ (in black, thin line) and $y_1(t)$ (in gray, thick line), respectively, at the beginning ($t\in[0,30]$) and at the end ($t\in[470,500]$) of the run [in Fig. 3(b) the two curves are superposed]. Figure 3(c) is a plot of the synchronization error $|x_1(t)-y_1(t)|$ versus t, from which we see that the adaptive strategy is successful in achieving synchronization between the true and the model systems. Figure 3(d) shows the time evolution of σ' converging to the true value of $\sigma=1$.

III. IDENTIFICATION OF DELAYS

Hereafter, we consider a completely different identification problem, in which the dynamics of the system to be identified is described by a set of delay differential equations,

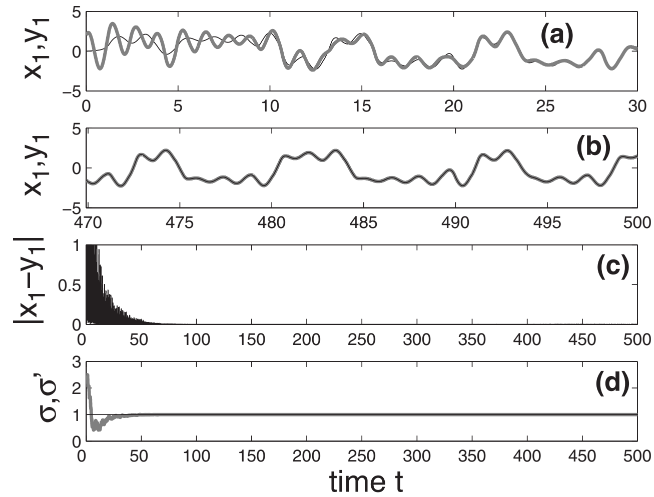

FIG. 3. (a) and (b) show the time evolutions of $x_1(t)$ (in black, thin line) and $y_1(t)$ (in gray, thick line) respectively at the beginning ($t\in[0,30]$) and at the end ($t\in[470,500]$) of the run [in (b) the two curves are superposed]. Plot (c) shows $|x_1(t)-y_1(t)|$ versus $t\in[0,500]$. As can be seen, after an initial transient, synchronization is achieved. (d) shows the time evolution of $\sigma'(t)$ (in gray), which converges to the true value of $\sigma=1$ [the σth ordinate line is plotted as a black thin solid line in (d)]. The true system obeys Eq. (12), $(\alpha,\beta,m_0,m_1)=(15.6,25.58,-8/7,-5/7)$, and the model system obeys Eq. (14), where the estimate σ' evolves according to Eqs. (16) and (18), $h(\mathbf{x})=x_1$, $\Gamma=[\gamma,0,0]^T$, $\gamma=15$, and $\zeta=1$. The initial conditions for the true and the model systems are randomly chosen points on the Chua double scroll attractor, σ' is evolved from an initial value that is far away from the true value of σ, i.e., $\sigma'(0)=2.5$, and $q_1(0)=0$.

$$\dot{\mathbf{x}}(t)=\Phi(\mathbf{x},\mathbf{x}_\tau,\mathbf{p}), \tag{19}$$

where $\mathbf{x}(t)=(x_1(t),x_2,(t)\ldots,x_n(t))^T$, $\mathbf{x}_\tau=\mathbf{x}(t-\tau)$, τ is a time delay, $\mathbf{p}=[p_1,p_2,\ldots,p_\ell]$ is a set of ℓ unknown parameters.

We try to model the dynamics of the true system by $\dot{\mathbf{y}}(t)=\Phi(\mathbf{y},\mathbf{y}_{\tau'},\mathbf{p}')$, where $(\tau',\mathbf{p}')$ are estimates of the unknown true coefficients $(\tau,\mathbf{p})$. Our goal is to evolve $(\tau',\mathbf{p}')$ in time to match the unknown true values of $(\tau,\mathbf{p})$ and in so doing, to achieve synchronization between the model and the true systems. We perform a one way diffusive coupling from the true system to the model, as follows,

$$\dot{\mathbf{y}}(t)=\Phi(\mathbf{y},\mathbf{y}_{\tau'},\mathbf{p}')+\Gamma[h(\mathbf{x})-h(\mathbf{y})], \tag{20}$$

where $h(\mathbf{x})$ and Γ are the same as defined before, $\mathbf{y}_{\tau'}=\mathbf{y}(t-\tau')$, $\mathbf{p}'=[p'_1,p'_2,\ldots,p'_\ell]$. In what follows, we assume for simplicity and without loss of generality that h is a scalar function, i.e., $m=1$. We now introduce the potential Ψ, defined in Eq. (15) (similar considerations apply as in the previous cases) and we propose to minimize Ψ by making $(\tau',p'_1,p'_2,\ldots,p'_\ell)$ converge onto the true values $(\tau,p_1,p_2,\ldots,p_\ell)$, through the following gradient descent relations,

$$\dot{\tau}'(t)=-\beta\frac{\partial\Psi}{\partial\tau'}=2\beta[h(\mathbf{y})-h(\mathbf{x})]Dh\mathbf{r}, \tag{21a}$$

$$\dot{p}_i'(t) = -\rho_i \frac{\partial \Psi}{\partial p_i'} = 2\rho_i[h(\mathbf{y}) - h(\mathbf{x})]Dh\mathbf{s}_i, \qquad (21b)$$

$i=1,\ldots,\ell$, $\beta,\rho_i>0$. We are now interested in how the n-vectors $\mathbf{r}=\partial\mathbf{y}'/\partial\tau'$, $\mathbf{s}_i=\partial\mathbf{y}'/\partial p_i'$ evolve in time. We note that the following *auxiliary* equations describe the evolution of $[\mathbf{r}(t), \mathbf{s}_i(t)]$, $i=1,\ldots,\ell$,

$$\dot{\mathbf{r}}(t) = \left[\frac{\partial \Phi(\mathbf{y},\mathbf{y}_{\tau'},\mathbf{p}')}{\partial \mathbf{y}} - \Gamma Dh\right]\mathbf{r} - \frac{\partial \Phi(\mathbf{y},\mathbf{y}_{\tau'},\mathbf{p}')}{\partial \mathbf{y}_{\tau'}}\dot{\mathbf{y}}_{\tau'}, \qquad (22a)$$

$$\dot{\mathbf{s}}_i(t) = \left[\frac{\partial \Phi(\mathbf{y},\mathbf{y}_{\tau'},\mathbf{p}')}{\partial \mathbf{y}} - \Gamma Dh\right]\mathbf{s}_i + \frac{\partial \Phi(\mathbf{y},\mathbf{y}_{\tau'},\mathbf{p}')}{\partial \mathbf{p}_i'}, \qquad (22b)$$

$\dot{\mathbf{y}}_{\tau'}=\dot{\mathbf{y}}(t-\tau')$. Therefore our adaptive strategy is fully described by the set of Eqs. (20), (21a), (21b), (22a), and (22b).

The above strategy is tested for a case, in which the true system is described by the Mackey-Glass equation, $n=1$, $\mathbf{x}(t)\equiv x(t)$, $\dot{x}=\phi(x,x_\tau,\mathbf{p})$,

$$\phi(x,x_\tau,a,b) = -bx(t) + ax_\tau/(1+x_\tau^{10}), \qquad (23)$$

Γ coincides with the scalar coupling γ. We choose $a=0.2$, $b=0.1$, $\tau=23$, and $h(x)=x$. For these values of the parameters, the dynamics of the Mackey-Glass system is chaotic.

We attempt to estimate the unknown delay τ and the unknown parameter a ($\ell=1$). Both the true system and the model systems are initialized from uniformly distributed random initial conditions on the chaotic attractor. We take $\beta=1$, $\rho_1=0.1$, and $\gamma=1$. The results of our numerical experiment are shown in Figs. 4(a)–4(c). The experiment consists of two parts. For $t\leq 10^5$, τ is kept constant and equal to 23, while τ' is initialized from a value that is far away from the true value of $\tau=23$, i.e., $\tau'(0)=15$ and $a'(0)=0.4$. As can be seen, after a transient, $t\gtrsim 4\times 10^4$, both τ' and a' converge to the true values of $\tau=23$ and $a=0.2$. For $10^5<t\leq 3\times 10^5$, τ becomes a function of time, i.e., $\tau(t)=23+2\sin(\pi 10^{-5}t)$, while the adaptive strategy [Eqs. (20), (21a), (21b), (22a), and (22b)] is kept running. As can be seen, for $t>10^5$, $\tau'(t)$ tracks quite well the time evolution of $\tau(t)$ and approximate synchronization between the model and the true system is attained. An important observation is that both the unknown parameters can be simultaneously extracted and from using the same source of information. We have also run another experiment, in which we were able to estimate the parameters a,b, and τ (not shown).

Figures 5(a) and 5(b) are plots of the average synchronization errors, respectively in the case of the Chua system and the Mackey-Glass system. (a) shows the average synchronization error $\langle|x_1-y_1|\rangle$ calculated from integration of Eqs. (12)–(14) versus σ' assumed *constant*, with the true value of σ having been set to 1. Fig. 5(b) shows $\langle|x-y|\rangle$ calculated from integration of Eqs. (19), (20), and (23) versus τ' assumed constant, with the true value of τ having been set to 23 ($a'=a=0.2$). The plotted synchronization errors are averaged over a long time and the initial transient, which reflects the choice of the initial conditions, is neglected. As can be seen, in both cases the average synchronization error is characterized by a sharp minimum at $\sigma'=\sigma=1$ ($\tau'=\tau=23$), and it rapidly increases with $|\sigma'-\sigma|$ ($|\tau'-\tau|$).

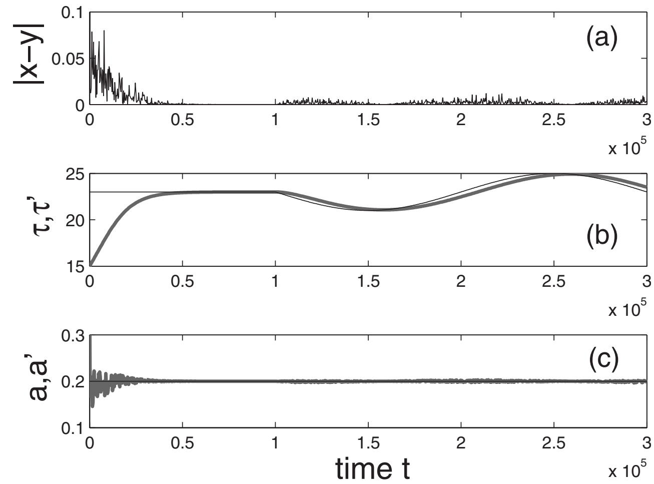

FIG. 4. Experiment with the Mackey-Glass system. (a) shows $|x-y|$ versus t. (b) shows the time evolution of $\tau'(t)$ (in gray, thick line), compared to the time evolution of $\tau(t)$ (in black, thin line). The experiment consists of two parts. In the first part, after an initial transient, the estimate τ' converges to the true value of $\tau=23$; in the second part, τ' tracks the time evolution of $\tau(t)=23+2\sin(\pi 10^{-5}t)$. (c) shows the time evolution of $a'(t)$ (in gray) converging to the true value of $a=0.2$ (in black, thin line). $\phi(x,x_\tau)=-0.1x+0.2x_\tau/(1+x_\tau^{10})$; $h(x)=x$, $\gamma=0.1$, $\beta=1$. The true system and the model system are initialized from uniformly distributed random initial conditions on the Mackey-Glass chaotic attractor.

IV. CONCLUSIONS

Synchronization of chaos has been shown to be a convenient tool to identify the dynamics of unknown systems. Different techniques have been proposed, see, e.g., [2–4]. Yet, the problems of identification of delays and discontinuity points that frequently characterize the dynamics of real systems have not received adequate attention. In this paper, we have proposed a fully nonlinear approach, based on a simple

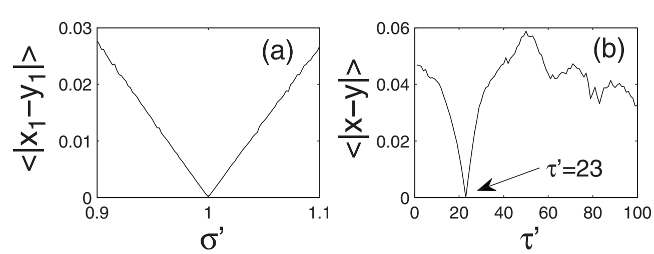

FIG. 5. (a) shows the average synchronization error $\langle|x_1-y_1|\rangle$ calculated from integration of Eqs. (12)–(14) versus σ' assumed constant, with the true value of σ having been set to 1. (b) shows $\langle|x-y|\rangle$ calculated from integration of Eqs. (19), (20), and (23) versus τ' assumed constant, with the true value of τ having been set to 23 ($a'=a=0.2$). The plotted synchronization errors are averaged over a long time and the initial transient is neglected. All the simulation parameters are the same as in Figs. 3 and 4.

gradient descent technique (MIT rule), to address both these problems. This strategy is completely described by integrable differential equations. We have also shown the usefulness of our strategy in the case that the unknown parameters of the true system to be estimated slowly drift in time. We successfully apply our methodology to solve problems as different as the identification of delays and the identification of discontinuity points of unknown dynamical systems. This suggests that our approach can provide a simple and flexible paradigm for the resolution of a variety of diverse identification problems.

ACKNOWLEDGMENT

The author is grateful to Ed Ott and Mario di Bernardo for insightful discussions.

[1] P. So, E. Ott, and W. P. Dayawansa, Phys. Rev. E **49**, 2650 (1994).

[2] H. D. I. Abarbanel, D. R. Creveling, and J. M. Jeanne, Phys. Rev. E **77**, 016208 (2008); J. C. Quinn, P. H. Bryant, D. R. Creveling, S. R. Klein, and H. D. I. Abarbanel, *ibid.* **80**, 016201 (2009).

[3] W. Yu, G. Chen, J. Cao, J. Lu, and U. Parlitz, Phys. Rev. E **75**, 067201 (2007).

[4] F. Sorrentino and E. Ott, Chaos **19**, 033108 (2009).

[5] B. Brogliato, *Impacts in Mechanical Systems: Analysis and Modelling* (Springer, Berlin, 2000).

[6] M. di Bernardo, K. H. Johansson, and F. Vasca, Int. J. Bifurcation Chaos Appl. Sci. Eng. **11**, 1121 (2001).

[7] S. Banerjee and G. C. Verghese, *Nonlinear Phenomena in Power Electronics: Bifurcations, Chaos, Control, and Applications* (Wiley-IEEE, New York, 2001).

[8] M. C. Mackey and L. Glass, Science **197**, 287 (1977).

[9] T. Erneux, *Applied Delay Differential Equations* (Springer, New York, 2009).

[10] A. G. Vladimirov, D. Turaev, and G. Kozyreff, Opt. Lett. **29**, 1221 (2004).

[11] V. Deshmukh, E. A. Butcher, and E. Bueler, Nonlinear Dyn. **52**, 137 (2008).

[12] S. Yi, P. W. Nelson, and A. G. Ulsoy, Math. Biosci. Eng. **4**, 355 (2007).

[13] N. Minorski, *Nonlinear Oscillations* (Van Nostrand, Princeton, 1962).

[14] L. A. Safonov, E. Tomer, V. V. Strygin, Y. Ashkenazy, and S. Havlin, EPL **57**, 151 (2002).

[15] T. Matsumoto, IEEE Trans. Circuits Syst. **31**, 1055 (1984).